Forcing mechanism of the seasonally asymmetric quasi-biennial oscillation secondary circulation in ERA-40 and MAECHAM5

C. Peña-Ortiz,[1] P. Ribera,[1] R. García-Herrera,[2] M. A. Giorgetta,[3] and R. R. García[4]

Received 15 August 2007; revised 7 April 2008; accepted 15 April 2008; published 21 August 2008.

[1] The seasonality of the quasi-biennial oscillation (QBO) and its secondary circulation is analyzed in the European Reanalysis (ERA-40) and Middle Atmosphere European Centre Hamburg Model (MAECHAM5) general circulation model data sets through the multitaper method-singular value decomposition (MTM-SVD). In agreement with previous studies, the results reveal a strong seasonal dependence of the QBO secondary circulation. This is characterized by a two-cell structure symmetric about the equator during autumn and spring. However, anomalies strongly weaken in the summer hemisphere and strengthen in the winter hemisphere, leading to an asymmetric QBO secondary circulation characterized by a single-cell structure displaced into the winter hemisphere during the solstices. In ERA-40, this asymmetry is more pronounced during the northern than during the southern winter. These results provide the first observation of the QBO secondary circulation asymmetries in the ERA-40 reanalysis data set across the full stratosphere and the lower mesosphere, up to 0.1 hPa. The MTM-SVD reconstruction of the seasonal QBO signals in the residual circulation and the QBO signals in Eliassen Palm (EP) flux divergences suggest a particular mechanism for the seasonal asymmetries of the QBO secondary circulation and its extension across the midlatitudes. The analysis shows that the QBO modulates the EP flux in the winter hemispheric surf zone poleward of the QBO jets. The zonal wind forcing by EP flux divergence is transformed by the Coriolis effect into a meridional wind signal. The seasonality in the stratospheric EP flux and the hemispheric differences in planetary wave forcing cause the observed seasonality in the QBO secondary circulation and its hemispheric differences.

Citation: Peña-Ortiz, C., P. Ribera, R. García-Herrera, M. A. Giorgetta, and R. R. García (2008), Forcing mechanism of the seasonally asymmetric quasi-biennial oscillation secondary circulation in ERA-40 and MAECHAM5, *J. Geophys. Res.*, *113*, D16103, doi:10.1029/2007JD009288.

1. Introduction

[2] *Ruzmaikin et al.* [2005] distinguished two different effects of the quasi-biennial oscillation (QBO) on extratropical latitudes. As originally found by *Holton and Tan* [1980], the polar night winds are weaker during the east phase of the QBO and stronger during its west phase. Holton and Tan suggested that the phase of the QBO in the tropics modulates the effective waveguide for planetary waves that propagate through the winter stratosphere driving the middle and high-latitude dynamics. The QBO signature induced in the planetary waves Eliassen Palm (EP) flux divergence induces anomalies in the middle- and high-latitude circulation and temperature of the winter hemisphere [*Tung and Yang*, 1994; *Hamilton*, 1998; *Ruzmaikin et al.*, 2005; *Calvo et al.*, 2007]. A second effect (explored in this paper) is based on seasonally asymmetric secondary circulation of the QBO that extends to midlatitudes in the winter hemisphere. Both effects involve extratropical planetary Rossby waves interaction with the QBO phases, which however has different effects in different latitudinal ranges and at different levels. The work by Holton and Tan focused on the effects in the high-latitude temperature and circulation. Our paper is focused on the effects in the subtropics and mid-latitudes in the vicinity of the QBO jets.

[3] It is well known that the equatorial zonal mean zonal wind jets of the QBO cause a secondary circulation. This *QBO secondary circulation* was first observed by *Reed* [1964]. In 1982, *Plumb and Bell* [1982] developed the first 2D model to analyze its latitudinal and vertical structure. This simulation and others performed later [*Dunkerton*, 1985; *Takahashi*, 1987] showed a secondary circulation characterized by rising (sinking) motions near the equator in zones of easterly (westerly) wind shear and meridional circulation branches extending to the subtropics and midlatitudes, forming symmetric circulation cells over both hemispheres.

[4] The studies mentioned above did not consider the modulation of the secondary circulation by the seasonal

[1]Departamento de Sistemas Fisicos, Quimicos y Naturales, Universidad Pablo de Olavide, Sevilla, Spain.
[2]Departamento de Física de la Tierra II, Facultad de CC Físicas, Universidad Complutense de Madrid, Madrid, Spain.
[3]Department of Atmosphere in Earth System, Max Planck Institute for Meteorology, Hamburg, Germany.
[4]Atmospheric Chemistry Division, National Center for Atmospheric Research, Boulder, Colorado, USA.

0148-0227/08/2007JD009288

cycle and others assumed that it was seasonally independent [*Holton*, 1989; *Tung and Yang*, 1994]. However, *Jones et al.* [1998], *Kinnersley* [1999], *Kinnersley and Tung* [1999] and *Ruzmaikin et al.* [2005] have demonstrated that the QBO secondary circulation is strongly dependent on season. These studies showed that, during solstice, the two-cell structure symmetric about the equator turns into one single cell displaced into the winter hemisphere. Circulation anomalies strengthen and expand, reaching extratropical latitudes in the winter hemisphere while they weaken or disappear from the summer hemisphere.

[5] In 1999, Kinnersley proposed a possible mechanism for the seasonal asymmetries of the QBO secondary circulation. *Kinnersley* [1999] suggested that the summer to winter mean circulation advects the equatorial zonal wind anomaly into the winter hemisphere reaching higher latitudes. The growth of the Coriolis parameter with latitude requires a larger temperature anomaly to maintain the thermal wind balance, which leads to a larger secondary circulation anomaly in the winter hemisphere. Therefore he could explain the seasonal asymmetries without invoking any interaction between the zonal wind and Rossby waves. He also suggested that the breaking and dissipation of Rossby waves causes the expansion of the circulation anomalies toward higher latitudes in the winter hemisphere.

[6] Here, the multitaper method-singular value decomposition (MTM-SVD) methodology [*Mann and Park*, 1999] has been applied to European Reanalysis (ERA-40) and Middle Atmosphere European Centre Hamburg Model (MAECHAM5) for each season separately in order to quantify the seasonality in the QBO and in its secondary circulation. We detect and reconstruct the asymmetric structure of the secondary circulation and suggest another possible mechanism for these asymmetries based on the interaction between Rossby waves and the QBO zonal wind.

2. Data

[7] Two different data sets have been used in this study: data from the ERA-40 reanalysis, prepared by ECMWF (European Centre for Medium Range Weather Forecasting; *Uppala et al.* [2005]), and from the MAECHAM5 model [*Manzini et al.*, 2006], which is the middle atmosphere configuration of the generic ECHAM5 general circulation model [*Roeckner et al.*, 2003, 2006] developed at the Max Planck Institute for Meteorology.

[8] ERA-40 resolves the atmosphere in 60 layers up to 0.1 hPa. While ERA-40 covers the time period of August 1956 to July 2002, we use for this study only the 21 year period of 1979 to 1999. The QBO is generally well represented in ERA-40 [*Baldwin and Gray*, 2005; *Pascoe et al.*, 2005], resulting from the assimilation of equatorial wind profiles [*Bengtsson et al.*, 2004].

[9] The MAECHAM5 version used in this study resolves the atmosphere in 90 vertical levels from the surface to 0.01 hPa ($\sim$80 km) altitude. In the stratosphere, the vertical resolution is approximately 700 m between the tropopause and 42 km height, and better than 1 km up to the stratopause. This vertical resolution permits the simulation of the QBO based on resolved and parameterized wave mean-flow interaction [*Giorgetta et al.*, 2002, 2006]. Sea surface temperature (SST) and sea ice distribution are prescribed as lower boundary conditions following the monthly climatology of the period 1979–1996 (AMIP2 data set), thus excluding atmospheric responses to El Niño or La Niña SST signals. Natural external forcings by major volcanic eruptions or by 11-year solar cycle variations of the irradiance are also neglected in the experiment. This experiment was integrated over 22 years, of which years 2 to 22 are evaluated, labeled for convenience as 1979 to 1999.

[10] For both data sets, monthly means of zonal wind, mass stream function based on the transformed Eulerian mean velocities v^* and w^*, Eliassen Palm (EP) flux components and divergence have been used. The residual circulation and EP flux was calculated from the Transformed Eulerian-Mean (TEM) equations based on the primitive equations [*Andrews and McIntyre*, 1976]. The data cover a 21-year period from 1979 to 1999. For ERA-40, 25 stratospheric and mesospheric levels from 96 to 0.1 hPa (96, 80, 61, 55, 44, 36, 29, 23, 19, 15, 12, 10, 8, 6, 5, 4, 3.36, 2.67, 2.08, 1.58, 1.15, 0.80, 0.51, 0.29, 0.10 hPa) have been analyzed using zonal mean data with a latitudinal resolution of approximately 1.1°. For MAECHAM5, a subset of 20 levels from 97 to 0.1 hPa (97, 74, 57, 44, 34, 27, 21, 16, 12, 9, 7, 5, 4, 3, 2, 1.46, 0.97, 0.61, 0.35 and 0.1 hPa) has been analyzed using zonal mean data with a latitudinal resolution of approximately 2.8°.

[11] Although the validation of the QBO in ERA-40 between 10 hPa and 1 hPa is difficult because of the shortage of observational data at these levels, the representation of the QBO signal is excellent up to 10 hPa [*Pascoe et al.*, 2005]. Recent studies show that ERA-40 provides a reliable representation of the QBO up to 2 hPa [*Baldwin and Gray*, 2005], though differences occur between the QBO in the upper stratosphere in earlier and later years of ERA-40 [*Punge and Giorgetta*, 2007]. For the purpose of this paper, ERA-40 results can be used as a reference to evaluate the QBO simulation in MAECHAM5. Further, a comparative analysis of the signal is used to validate coherent patterns in both data sets.

3. Methodology

[12] The method applied in this study is the multitaper frequency-domain singular value decomposition or "MTM-SVD" [*Mann and Park*, 1999]. The MTM-SVD approach detects and reconstructs statistically significant narrowband oscillations that are correlated among a sufficiently large number of normalized independent series (e.g., time series of wind at different locations). The quasi-oscillatory property of the QBO therefore makes this method suitable for analyzing the QBO structure or QBO related signals.

[13] The application of this method is based on a multitaper spectral analysis (MTM) followed by singular value decomposition (SVD). Each standardized time series for each grid point is Fourier transformed from the time to the frequency domain using the MTM procedure. The resultant coefficients and phase information for each frequency are organized into different matrices, which undergo a complex SVD. The first mode eigenvalues explain the maximum variance associated with the first eigenvectors obtained for each frequency, that is, the local fractional variance. These eigenvalues are plotted against the frequency to construct the local fractional variance spectrum (LFV spectrum). This

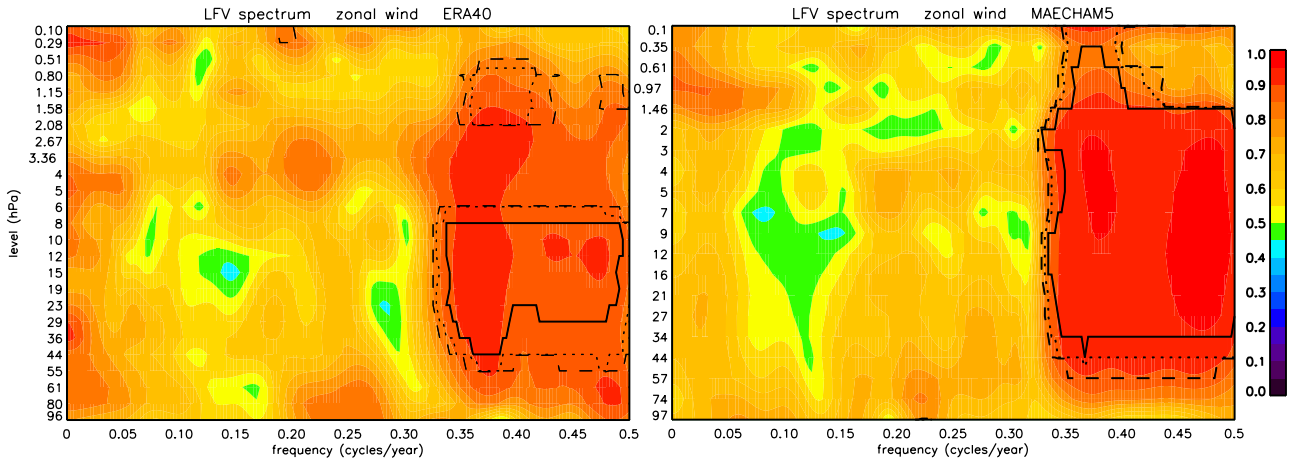

Figure 1. LFV spectra obtained for the monthly mean zonal wind for ERA-40 and MAECHAM5 data. The color scale represents the variability associated to the first eigenvalue for each frequency and level. Levels of significance are represented through a solid line (99 %), dotted line (95 %), and dashed line (90 %).

provides a powerful frequency domain signal detection parameter, indicating the maximum fraction of narrowband spatiotemporal variance that can be explained by a particular modulated oscillation as a function of frequency [*Mann and Park*, 1999]. A bootstrap method [*Efron*, 1990] is used to determine statistical significance levels. One thousand different combinations of the temporal intervals are used to generate one thousand randomized versions of the analyzed field, which conserve the spatial but not the temporal structure. Statistical significance levels are thus obtained by taking the 90%, 95% and 99% percentiles of this set of fields. Once the signal is detected in the spectrum, a frequency is chosen to reconstruct its spatial pattern from the complex first eigenvector, which contains information about relative phase and amplitude of the signal at all locations. This is done for different phases of the oscillation in order to obtain its evolution through a complete cycle. Previous analysis of the QBO based on this method can be found in the work of *Ribera et al.* [2003, 2004].

[14] In this study the original time series have been converted into seasonal means. Thus the winter series corresponds to the mean of December, January and February (DJF) for each year, the spring series to the mean of March, April and May (MAM), the summer series to June, July and August (JJA) and the autumn series to the mean of September, October and November (SON). The MTM-SVD has been applied to these seasonal series separately so that the annual cycle does not enter directly the MTM-SVD analysis. This procedure permits the reconstruction of the QBO patterns associated with each season to detect the annual cycle modulation of the QBO signal. More details about the application of this methodology can be found in the work of *Ribera et al.* [2004], where the same procedure was followed to reconstruct the secondary circulation in monthly mean time series, neglecting the seasonal dependence.

4. Results

4.1. Detection of the QBO Signature: LFV Spectra

[15] With the aim of identifying the QBO signal and analyzing its statistical significance in ERA-40 and MAECHAM5 data sets, LFV spectra were constructed for each variable (zonal wind, mass stream function and EP flux divergence) at each stratospheric level including all latitudes.

[16] Figure 1 represents the LFV spectra obtained for monthly mean time series of zonal mean zonal wind from ERA-40 and MAECHAM5. Highly significant peaks can be distinguished in the frequency band between 0.35 and 0.5 cycles/year, equivalent to a period ranging from 24 to 34 months, at several stratospheric levels. This band coincides with the frequency range of the QBO [*Baldwin et al.*, 2001]. Significant peaks above 99% are found between 50 hPa and 6 hPa for ERA-40 and between 45 hPa and 2 hPa for MAECHAM5, the atmospheric layer where the zonal wind variability of the equatorial region is dominated by the QBO [*Baldwin et al.*, 2001]. These spectra make evident the existence of the QBO signature in both data sets and the ability of the MTM-SVD to detect the signal. The reconstruction of the QBO signature from monthly mean time series through the MTM-SVD was analyzed by *Ribera et al.* [2003, 2004].

[17] For the reconstruction of the QBO patterns corresponding to each season, the LFV spectra were also reconstructed separately for winter, spring, summer and autumn time series. Figure 2 depict the winter (DJF) spectra for ERA-40 (left column) and MAECHAM5 (right column). In all cases the frequency band between 0.35 and 0.5 cycles/year, equivalent to a period ranging from 24 to 34 months, is characterized by highly significant peaks at several levels. This band coincides with the frequency range of the QBO [*Baldwin et al.*, 2001]. In the zonal wind spectra, significant peaks above 95% are found between 60 and 1 hPa approximately, the atmospheric layer where the zonal wind variability of the equatorial region is dominated by the QBO [*Baldwin et al.*, 2001].

[18] Despite the small magnitude of the QBO anomalies in the residual circulation [*Huesmann and Hitchman*, 2001; *Ribera et al.*, 2004] the QBO signal is also detected in the LFV spectra obtained for the mass stream and the EP flux divergence (Figure 2), with the QBO arising as the most intense quasi-oscillatory signal for all variables.

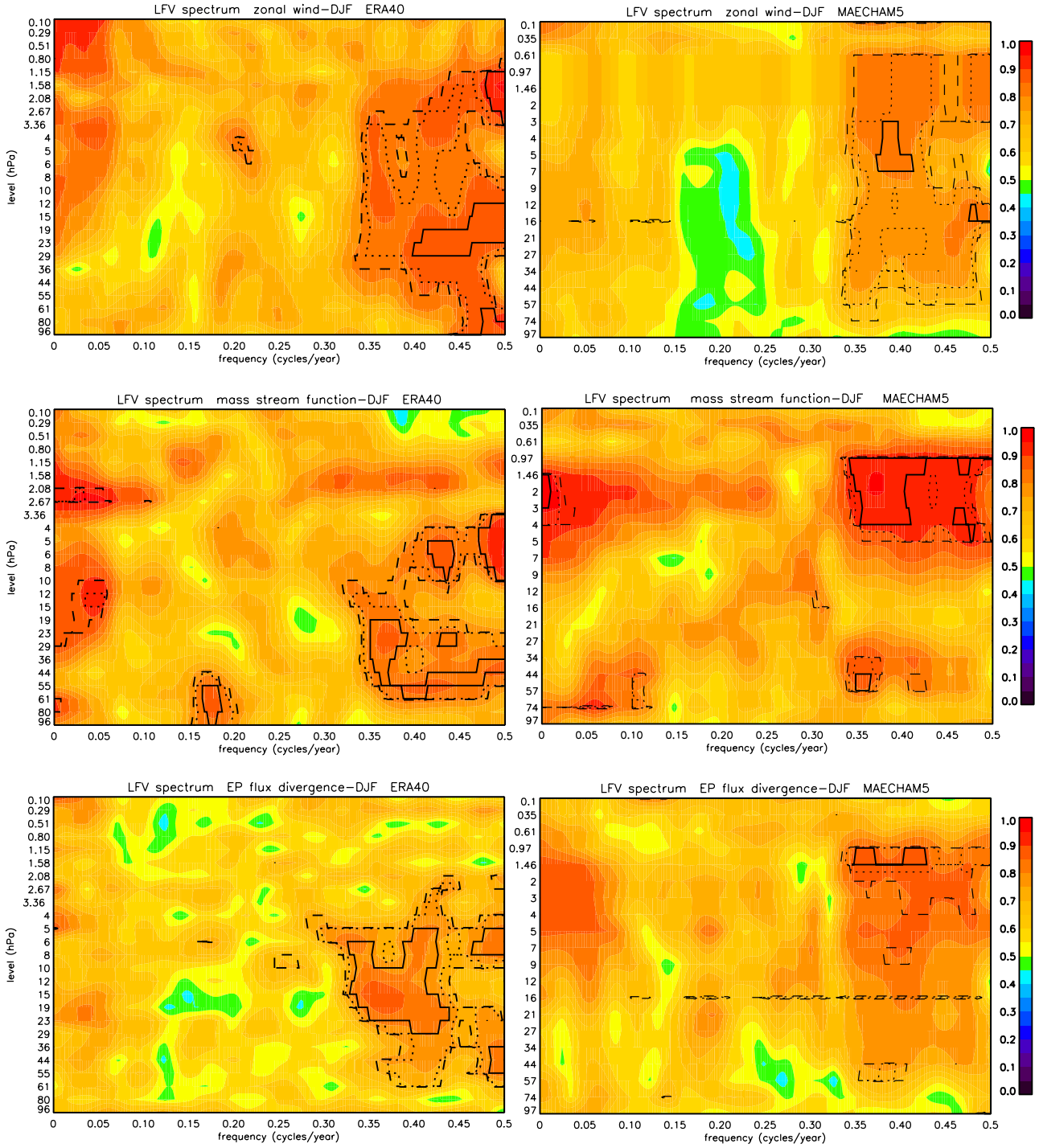

Figure 2. Same as Figure 1 but for the winter (DJF) zonal wind, mass stream function, and EP flux divergence.

[19] Similar results were obtained for spring and autumn for both data sets (not shown). However, in these seasons the QBO is more clearly detected in MAECHAM5 data than in ERA-40. This difference becomes more noticeable in northern hemisphere summer, when no significant peaks in the QBO frequencies are found for ERA-40 data while they are detected for MAECHAM5. ERA-40 reanalysis data are based on observations and, as a consequence, contain more complex variability and more intense climatic noise, which makes the detection of the signal more difficult. This fact can explain why the QBO can be more clearly identified in MAECHAM5, where the boundary conditions are less complex.

[20] Once the QBO signal has been detected, the patterns associated with the QBO frequencies are reconstructed in order to analyze the spatial structure of the signal. The patterns for several frequencies of the interval between 0.35 and 0.5 cycles/year were reconstructed (not shown) in order

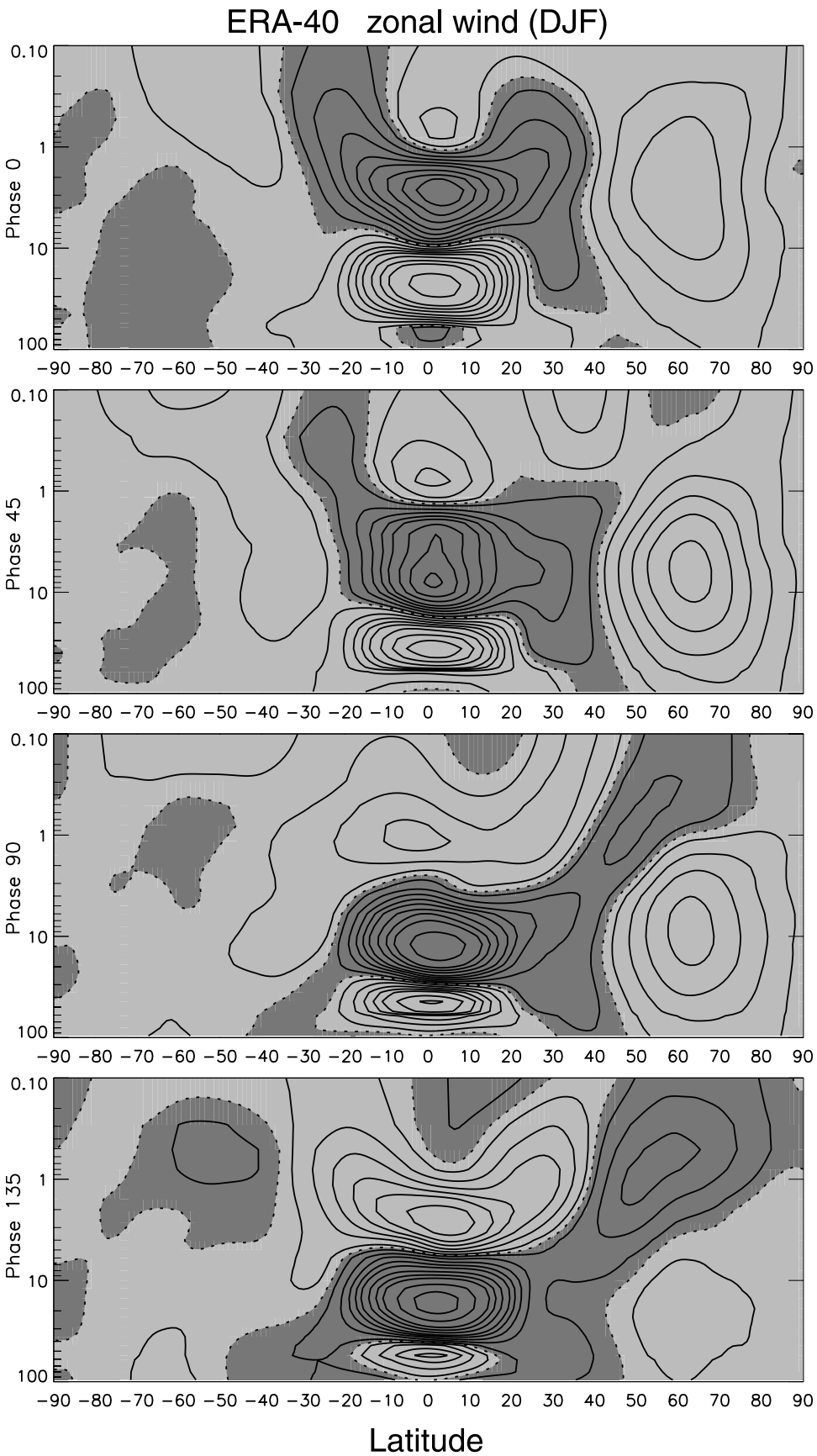

Figure 3

to confirm the consistency between the obtained patterns. Consistent results were obtained with the other frequencies and only some discrepancies in the magnitude of the anomalies but not in their spatial structure were found for the frequencies closer to the extremes of the frequency band. The patterns shown in this paper correspond to 0.40 cycles year^{-1}, equivalent to a 30-months period. They have been reconstructed for 8 consecutive phases of a complete QBO cycle in intervals of 45° (0°, 45°, 90°, 135°, 180°, 225°, 270° and 315°) where phase 0° corresponds to the westerly phase centered at 30 hPa and phase 180° to the easterly phase centered at 30 hPa. Anomalies at 180°, 225°, 270° and 315° are by construction opposite to those at 0°, 45°, 90° and 135°. Since the spatial reconstruction has been performed separately for each season, the reconstructed spatial patterns shows for a given season the typical structure of the QBO signals at QBO phase intervals of 45° (This must not be confused with a sequence of QBO signals at 45° phase intervals of a contiguous QBO cycle, which would spread across the seasons in approximately 3.7 month intervals.) The reconstructed patterns show the spatial structure of anomalies in the respective variables from their seasonal climatological mean for different phases of the QBO zonal wind anomalies occurring in the selected season. As an example, Figure 3 represents the ERA-40 zonal wind pattern associated with 0.40 cycles yr^{-1} for DJF. It shows the latitude-height structure of the QBO anomalies at four different phases from 0° to 135°. We defined phase 0° as QBO westerlies centered at 30 hPa. At phase 45° westerlies are centered at around 40 hPa. At phases 90° and 135° strong easterlies are found centered around 15 hPa and 20 hPa.

[21] In the next sections we generally are going to use phase 135° (easterlies centered at 15 hPa) to show our results. This phase was chosen to minimize the QBO signature because of the Holton and Tan (H-T) relationship which is weaker at this phase. Anomalies induced at middle and high latitudes through the H-T mechanism could make more difficult to identify the extratropical QBO signature because of the seasonal asymmetry of the secondary circulation of the QBO.

4.2. Seasonality in the QBO Zonal Wind

[22] The spatial patterns of the zonal wind anomalies associated with 0.40 cycles yr^{-1} have been reconstructed for each season separately. The common vertical domain of the ERA-40 and MAECHAM5 data, reaching 0.1 hPa, allows the reconstruction of the signal throughout the entire stratosphere and lower mesosphere. Figure 4 shows the zonal wind patterns at phase 135° obtained for each season and for ERA-40 (left) and MAECHAM5 (right) respectively. A more detailed description of the QBO in ERA-40 and MAECHAM5 can be found in the works of *Pascoe et al.* [2005] and *Giorgetta et al.* [2006], respectively, where the seasonality of the QBO vertical phase structure was excluded.

[23] The QBO vertical phase structure depicted in Figure 4 presents very similar characteristics in all seasons. However, a slight displacement of westerlies and easterlies toward the winter hemisphere during the solstices (Figure 4, first and third row) can be seen. This seasonal asymmetry has been previously observed [*Dunkerton and Delisi*, 1985, 1997] and obtained in a model simulation [*Dunkerton*, 1997]. Here the patterns obtained with both ERA-40 and MAECHAM5 data show that the maximum wind oscillation moves 2° or 3° of latitude into the winter hemisphere and that, westerly and easterly jets reach higher latitudes in the winter hemisphere. This is more evident above 5 hPa, where QBO anomalies of 5 m/s reach 30° of latitude in the northern winter hemisphere but only 20° in the southern summer hemisphere. During JJA, anomalies extend less to the subtropics of both hemispheres, and the difference between the winter and the summer hemisphere is not as significant as for DJF.

[24] A reason for this asymmetry was proposed by *Kinnersley* [1999]. The summer to winter mean circulation may advect the equatorial zonal wind anomaly into the winter hemisphere. This meridional circulation is more intense above 5 hPa, where an important region of planetary waves breaking is located. Additionally, the meridional circulation is stronger in the northern winter because of a greater planetary wave activity. This can explain the more evident displacement of zonal wind anomalies into the winter hemisphere in the upper stratosphere and in the northern winter hemisphere.

4.3. Seasonality of the QBO Secondary Circulation

[25] To study the seasonality of the QBO signal in the residual circulation the spatial patterns of the mass stream function based on the transformed Eulerian mean velocities v^* and w^* have been reconstructed for each season. Figure 5 shows the results obtained for ERA-40 and MAECHAM5 data, respectively. The displayed spatial patterns are associated with the QBO at phase 135°. Light and dark shading indicate clockwise and counterclockwise circulation respectively.

[26] The secondary circulation associated with the QBO can be clearly distinguished in both data sets. The differential latitudinal deflection of the zonal wind at the equator (beta effect) causes meridional convergence or divergence and, by continuity, vertical motion. These motions give rise to the circulation cells typical of the QBO secondary circulation (Figure 5). These QBO related anomalous meridional circulation cells modify transport paths of tracers in the middle atmosphere. However, these anomalous meridional circulation cells seen in the mass stream function must not be interpreted as Lagrangian circulations trajectories.

[27] In agreement with previous studies [*Jones et al.*, 1998; *Kinnersley*, 1999] the results reveal a strong seasonal dependence of the QBO secondary circulation. Mass stream function anomalies in the tropics and subtropics show a larger degree of symmetry during the equinoxes leading to a secondary circulation characterized by a two-cell structure

Figure 3. Reconstructed zonal wind pattern associated with 0.40 cycles year^{-1} for winter (DJF) data from the ERA-40 data set. The pattern is represented at four different phases from 0° (QBO westerlies centered at 30 hPa) to 135° in intervals of 45° as a function of latitude and pressure. Contours are drawn at ±0, 1, 3, 5, 7, 9, 12, 15, 18, 24, and 30 m/s. Light (dark) gray denotes positive (negative) anomalies.

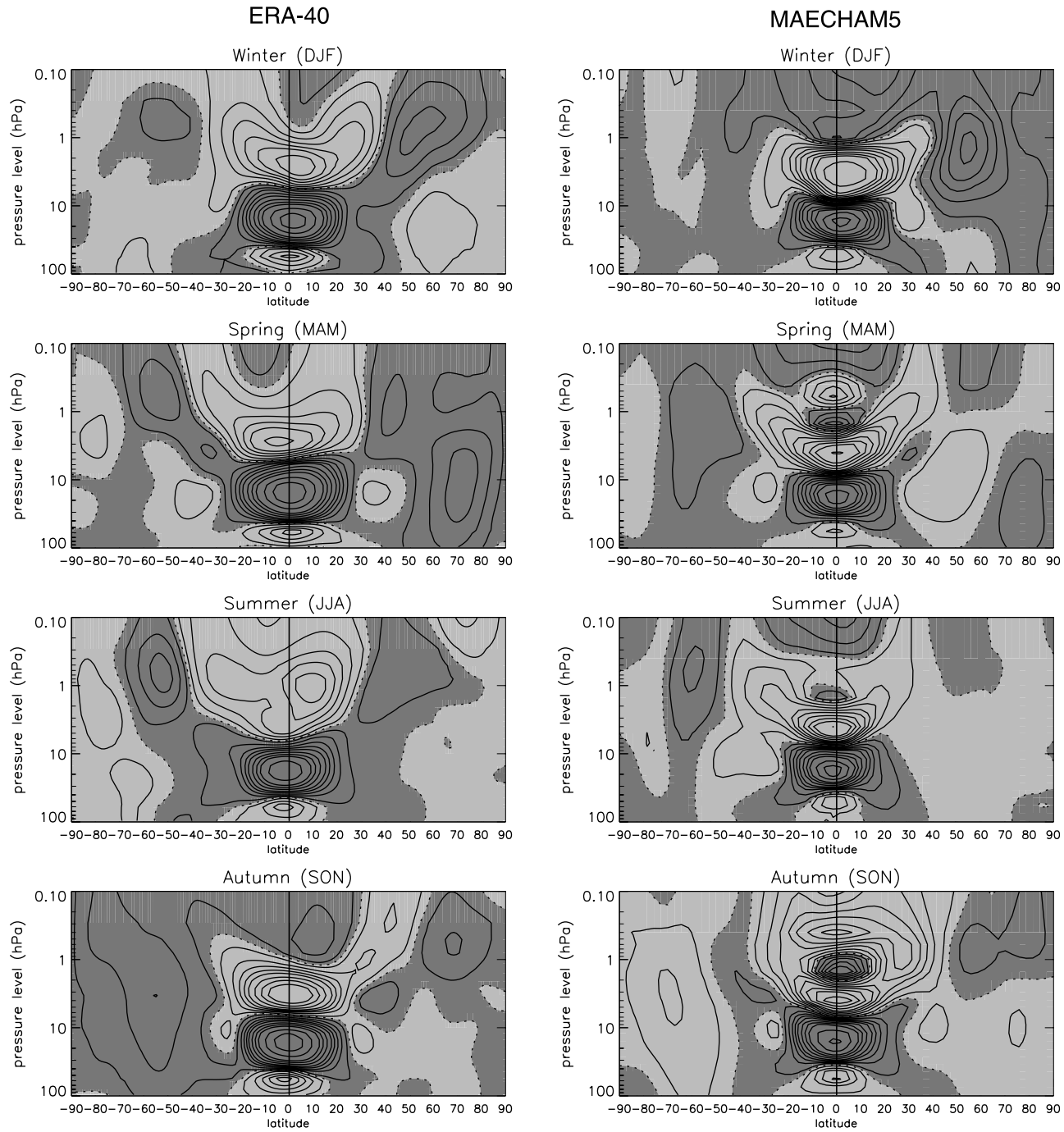

Figure 4. Reconstructed zonal wind patterns associated with 0.40 cycles year^{-1} at phase 135° (easterlies centered at around 15 hPa) for each season and for (left) ERA-40 and (right) MAECHAM5, respectively. Contours are drawn at ±1, 3, 5, 7, 9, 12, 15, 18, 24, and 30 m s^{-1}. Light (dark) gray denotes positive (negative) anomalies.

nearly symmetric about the equator. Such structures are also obtained in similar analyses conducted for all months of the time series at once [*Ribera et al.*, 2004]. However, during solstices circulation cells of the summer hemisphere weaken while they strengthen in the winter hemisphere.

[28] ERA-40 results for spring and autumn (Figure 5, left column) show a secondary circulation characterized by two pairs of circulation cells located at successive levels from 60 hPa to 3 hPa. A weaker third pair of cells is also observed above 3 hPa in both patterns and part of another one can be distinguished below 60 hPa. Both, autumn and spring patterns show a high degree of equatorial symmetry throughout the entire stratosphere. The strength and also the latitudinal extension of the cells are very similar in both hemispheres. Mass stream function anomalies in the low stratosphere are higher than 10^9 kg s^{-1}. Anomalies decrease with height reaching maximum values around 5×10^8 kg s^{-1} in the second pair of cells. Anomalies

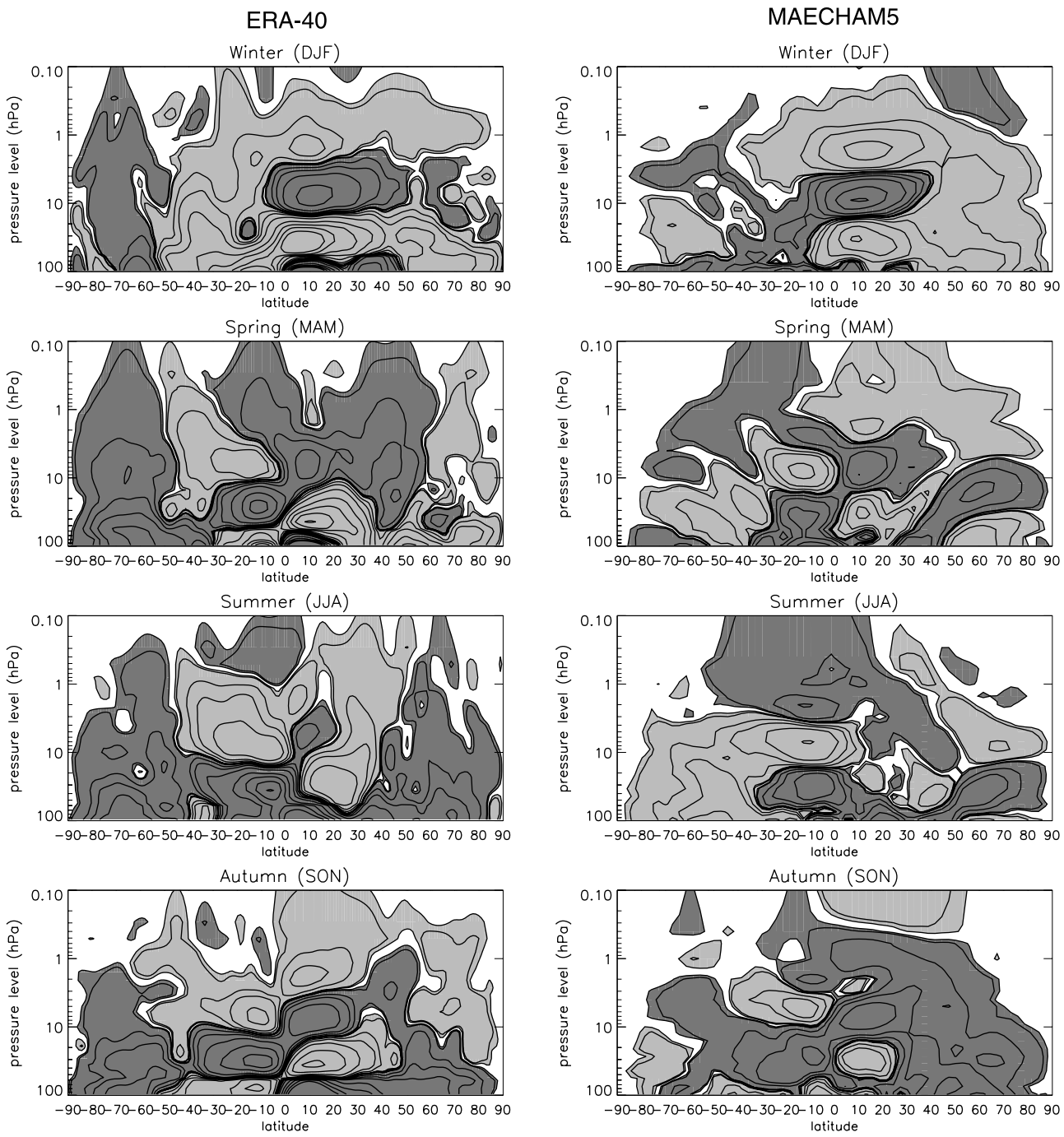

Figure 5. Reconstructed mass stream function patterns associated with 0.40 cycles year^{-1} at phase 135° for each season and for (left) ERA-40 and (right) MAECHAM5, respectively. Contours are drawn at ±5, 10, 50, 100, 200, 400, 600, 800, and 1000 × 10^6 kg s^{-1}. Light (dark) gray denotes clockwise (counterclockwise) anomalies.

above 3 hPa are not higher than 5 × 10^7 kg s^{-1}. The latitudinal extension of the cells also varies with height. However, generally, anomalies strongly decrease at 35°–40° of latitude.

[29] The QBO secondary circulation pattern turns greatly asymmetric during the northern winter (Figure 5, left column, first row). Circulation cells nearly disappear from the summer hemisphere while those in the winter hemisphere intensify and extend to higher latitudes. The vertical structure of the secondary circulation during the westerly QBO phase is characterized by three circulation cells in the winter hemisphere that alternate at consecutive levels up to 0.1 hPa. The latitudinal extent of the winter cells reaches here 45°–50° of latitude and anomalies at 30° and higher latitudes are stronger than in the patterns obtained for the equinoxes.

[30] In ERA-40 the hemispheric asymmetry of the QBO secondary circulation is less intense during the southern

winter (Figure 5, left column, third row). Mass stream function anomalies in the extratropical southern winter hemisphere are slightly weaker than those obtained in the northern winter hemisphere and circulation cells are stronger in the northern than in the southern summer hemisphere. Although the asymmetry is always evident, patterns obtained for different phases of the QBO cycle (not shown) show that the degree of asymmetry of the secondary circulation can vary with the vertical phase structure of the QBO during the southern summer (JJA).

[31] The magnitude of the stratospheric mass stream function due to the annual cycle in ERA-40 it is of the order of 10^9 kg s^{-1} but for the northern winter when it can be above 10^{10} kg s^{-1} in the winter hemisphere. Hence QBO anomalies represent between 1% and 10 % of the magnitude of the stratospheric residual circulation.

[32] The seasonal dependence of the secondary circulation of the QBO is also evident in the patterns obtained with MAECHAM5 data (Figure 5, right column). They show a vertical structure characterized by circulation cells that are symmetric about the equator in spring and autumn and asymmetric in summer and winter seasons.

[33] In spring and autumn (Figure 5, right column, second and fourth row), three pairs of circulation cells nearly symmetric about the equator can be clearly identified at consecutive levels between 100 hPa and 1 hPa. Very small anomalies give rise to one more pair between 1 and 0.5 hPa in the spring pattern. The largest anomalies, reaching values higher than 2×10^8 kg s^{-1}, are found in the two lower pair of cells.

[34] The northern and southern winter patterns obtained with MAECHAM5 (Figure 5, right column, first and third row), show a QBO secondary circulation totally asymmetric. Three circulation cells are observed in the winter hemispheres extending above 1 hPa while they have almost disappeared from the summer hemispheres. Comparing the circulation cells of the winter hemispheres with those obtained for spring and autumn important differences appear in the middle and upper stratosphere. There, both the strength and the latitudinal extension of the cells are greater in winter than in autumn or spring.

[35] In general, ERA-40 and MAECHAM5 results show a high level of consistency. However, some differences in the spatial structure of the QBO secondary circulation are also observed. The vertical extent of the cells is smaller in MAECHAM5 than in ERA-40, which is in agreement with the QBO zonal wind structure in MAECHAM5. QBO mass stream function anomalies are less intense in MAECHAM5, mainly in the lower stratosphere, where the jets have a smaller meridional width (cf. discussion in section 3b of *Giorgetta et al.* [2006]). Finally, the hemispheric asymmetries during the solstices are more pronounced in MAECHAM5 than in ERA-40. In MAECHAM5 the circulation cells disappear from the summer hemisphere during both the southern and northern winter while in ERA-40, anomalies still remain during the southern winter when the asymmetries are not as strong as during the northern winter.

[36] The secondary circulation of the QBO has been previously detected through its effects on the distribution of several dynamic variables and tracers; however, the small magnitude of the vertical and meridional wind involved makes its direct observation difficult. *Huesmann and Hitchman* [2001] published the first direct observation of the QBO secondary circulation in a global meteorological data set, the NCEP/NCAR reanalysis with a vertical coverage that up to 10 hPa. Our study extends their analysis to higher levels by use of the ERA-40 reanalysis reaching up to 0.1 hPa. It offers a clear picture of the secondary circulation in ERA-40 that shows QBO anomalies in the residual circulation through the entire stratosphere and also above 1 hPa, where, however, they must be interpreted with caution because of the vicinity of the upper boundary of the GCM used in the ERA-40 reanalysis. The seasonal asymmetries of the circulation anomalies in the meridional plane are evident in both ERA-40 and MAECHAM5 results.

4.4. Forcing Mechanism of the Seasonally Asymmetric QBO Secondary Circulation

[37] In order to analyze the zonal mean flow and the residual circulation response to eddy forcing, the Transformed Eulerian-Mean (TEM) equations based on the primitive equations [*Andrews and McIntyre*, 1976] are used. From these equations it can be deduced that, in the tropical area, where rotational effects are weak and the Coriolis parameter is small, the primary response to the eddy forcing will be a local acceleration of the mean zonal wind. However, outside this region, the Coriolis force substantially cancels the eddy forcing due to a mean meridional circulation [*Lindzen and Holton*, 1968; *Haynes*, 1998], at least on the long time scales under consideration here [see, e.g., *Garcia*, 1987]. Following this reasoning, *Haynes* [1998] stated that the latitudinal scale of the QBO could then be determined by the transition from the tropical to the extratropical regime and not by the latitudinal width of the momentum fluxes of particular wave types or wave source regions.

[38] In this section we analyze a possible mechanism for the seasonal dependence of the QBO secondary circulation. For that purpose the QBO signature in the EP flux divergence is investigated through the reconstruction of the EP flux divergence spatial patterns associated with the QBO frequency for each season. In MAECHAM5, wave-mean flow interaction includes both resolved waves, up to the truncation limit at wave number 42 in our experiment, and the parameterized effects of the interaction of gravity waves with the resolved wind. The resolved wave-mean flow interaction is diagnosed as the divergence of the EP flux while the parameterized gravity wave drag is directly accessible within the GCM integration [*Giorgetta et al.*, 2006]. These waves have different sources and may dissipate in different regions. Thus in order to evaluate the residual circulation response to the eddy forcing, we have reconstructed the patterns for EP flux divergence and also for the gravity wave drag simulated in MAECHAM5.

[39] In ERA-40, the circulation is determined by the dynamics of the GCM and by the assimilation of the observed meteorological fields. Gravity wave drag from tropospheric wave sources is neglected in the GCM used for ERA-40. In ERA-40, the resolved wave mean-flow interaction is assessed by EP flux divergence, as in MAECHAM5 simulation. However, there is no possibility to assess the effects of unresolved waves; since it is unclear to

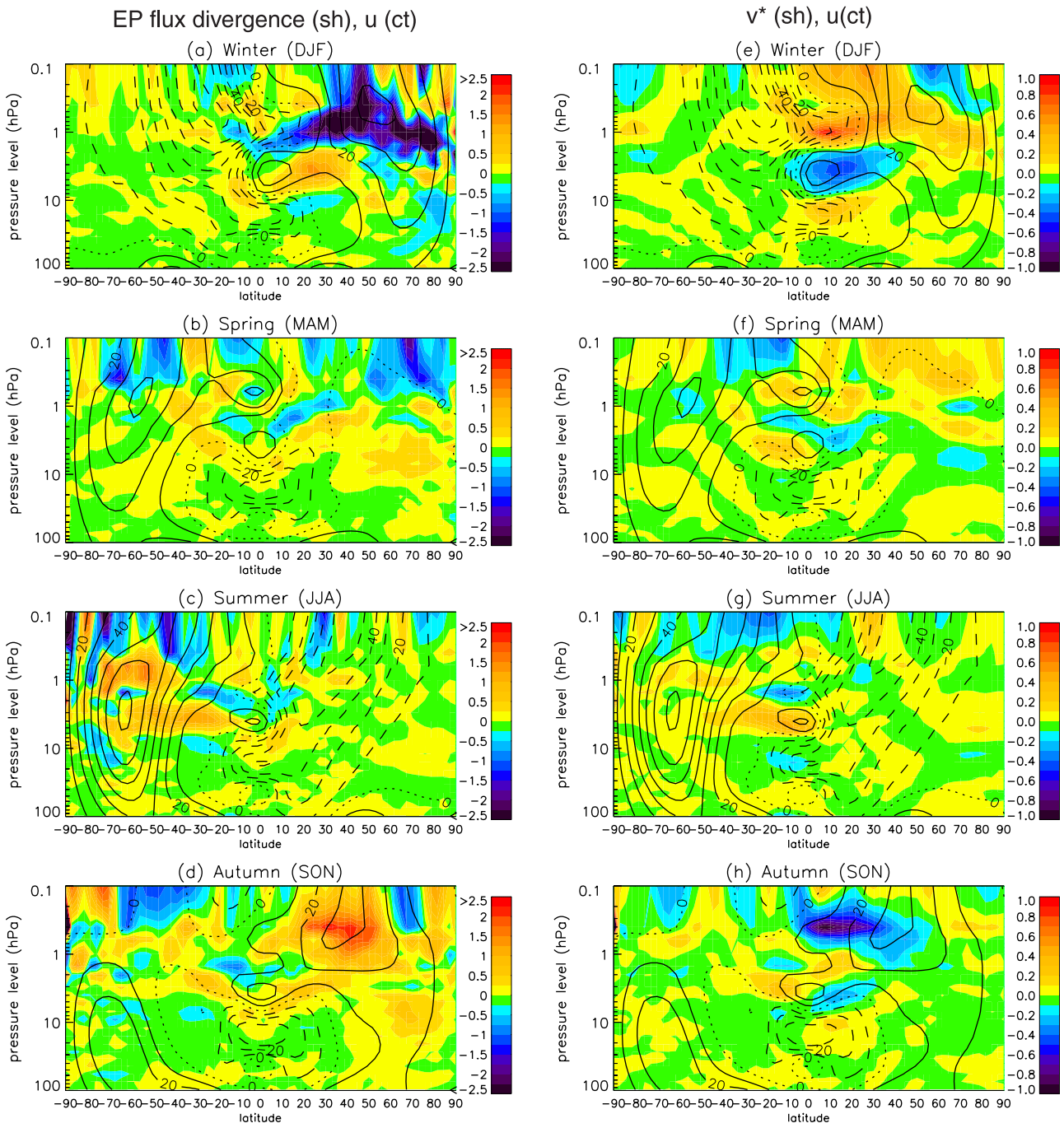

Figure 6. The left column shows the EP flux divergence patterns associated with 0.40 cycles/year at phase 135 for (a) winter, (b) spring, (c) summer, and (d) autumn; their magnitude is indicated by the color scale. On the right column, the color scale represents the v^* pattern for (e) winter, (f) spring, (g) summer, and (h) autumn. The contour lines represent the total zonal mean wind field, that is, the QBO zonal wind anomalies plus the winter mean zonal wind. Contour lines are drawn at intervals of 10 m s^{-1}. The dotted line is the zero wind line. Solid (dashed) line denotes positive (negative) anomalies.

what degree their effects are captured by the assimilation system.

[40] Here, after having validated the representation of the QBO secondary circulation in MAECHAM5, the mechanism for the seasonal dependence of the QBO secondary circulation is primarily analyzed in the model simulation. Since the model evolves under internally computed tendencies of the resolved dynamics and parameterized processes, the origin of the resulting dynamics should be clearer than in ERA-40 data, which include modeled tendencies and increments based on observations.

[41] EP flux divergence and meridional wind anomalies associated with the QBO are represented in Figures 6 and 8 for MAECHAM5 and ERA-40, respectively. These figures

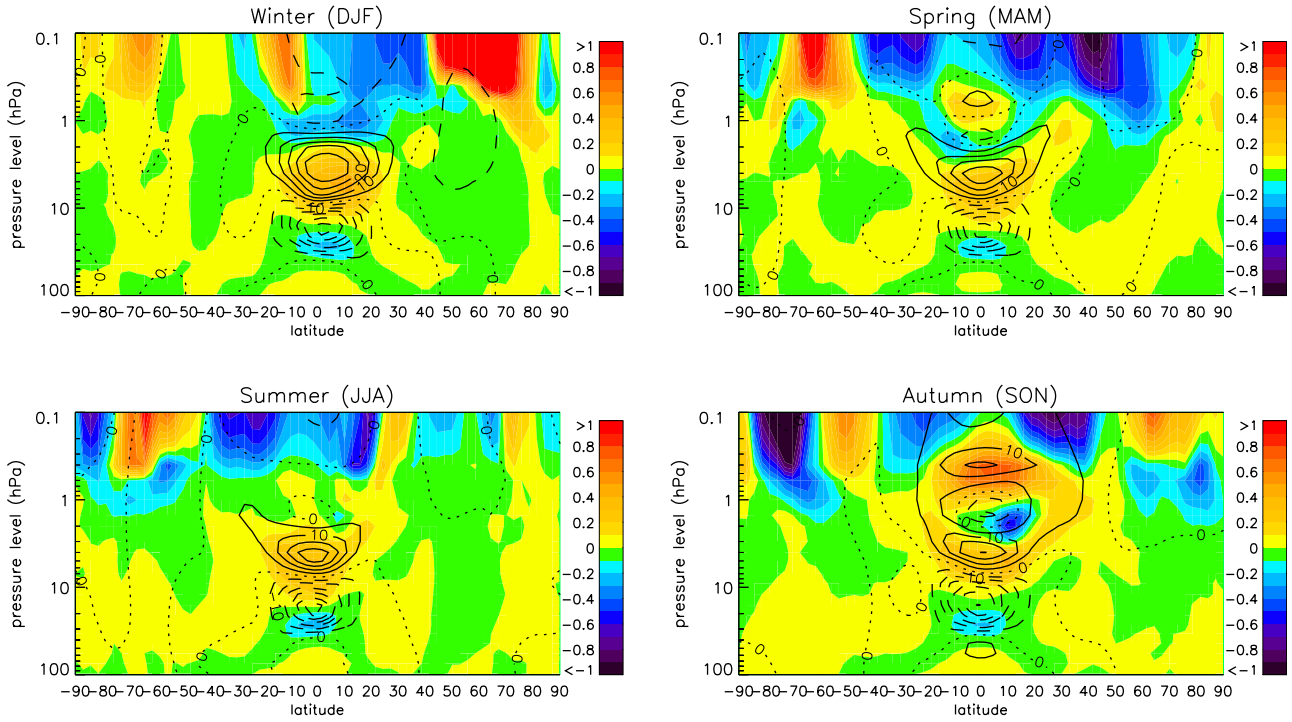

Figure 7. Reconstructed d*u*/d*t* due to gravity wave drag (m s^{-1} day^{-1}) patterns associated with 0.40 cycles $year^{-1}$ at phase 135° for MAECHAM5 data. The color scale represents gravity wave drag anomalies. Although anomalies reach 5 m s^{-1} day^{-1} in the extratropics, they are never larger than 1 m s^{-1} d^{-1} in the tropical region, which is our area of interest. The contour lines represent QBO zonal wind anomalies. Contours are drawn at intervals of 5 m s^{-1}. Solid (dashed) line denotes positive (negative) anomalies.

show the results obtained for winter, spring, summer and autumn. Contour lines represent the total reconstructed wind, that is, the sum of the reconstructed QBO zonal wind anomalies plus the mean zonal wind for each season. These figures correspond to the 135° phase of the QBO patterns; that is, to QBO easterly wind centered at 15 hPa.

[42] The patterns obtained for each season reveal a marked seasonal dependence in the eddy forcing associated with the frequency of 0.4 cycles per year that is characteristic for the QBO. EP flux divergence and convergence anomalies form slant bands extending from the shear layers of the QBO to levels and latitudes north and/or south of the zonal wind jets of the QBO. These arc-like structures in the tropical region alternate in the vertical corresponding to equatorial westerly and easterly shear zones and jets of the QBO. The structures in the QBO shear layers are expected from the dissipation of upward propagating equatorial waves with positive/negative phase velocity at westerly/easterly shear zones [*Plumb*, 1984]. The EP flux anomalies extend to higher latitudes and strengthen in the extratropics of the winter hemisphere, while they weaken in the summer hemisphere. Therefore EP flux divergence anomalies are approximately symmetric about the equator in spring and autumn and asymmetric in summer and winter in the same way as for the secondary circulation associated with the QBO.

[43] Figures 6a and 6c show MAECHAM5 patterns for the EP flux divergence during winter and summer. The asymmetric structure of the anomalies is evident for these seasons. While positive (negative) anomalies associated with westerly (easterly) shear zones extend to 20° latitude in the summer hemisphere, they extend beyond 50° latitude in the winter hemisphere. On the other hand, Figures 6b and 6d depict the pattern for spring and autumn, when the EP flux divergence anomalies form an arc-like structure nearly symmetric about the equator. In the tropical region the anomalies reach values of around 0.5 m s^{-1} d^{-1} in every season. However, at extratropical latitudes, anomalies are much larger in the winter hemisphere, especially in the northern winter when they reach values around 1.5 m s^{-1} d^{-1} between 5 and 3–2 hPa. They are slightly weaker in the southern winter hemisphere.

[44] Figure 7 shows the gravity wave drag patterns associated with the QBO for each season. As expected, positive (negative) anomalies are found at westerly (easterly) shear zones. These anomalies are slightly shifted into the winter hemisphere which is consistent with the QBO zonal wind displacement during the solstices (Figure 4). The summer-to-winter mean circulation may advect the QBO into the winter hemisphere, thus allowing gravity waves to interact with the QBO zonal wind at higher latitudes in that hemisphere. Thus gravity waves also generate an asymmetric forcing about the equator during the solstices. Comparing these results with MAECHAM5 patterns for the EP flux divergence, it is evident that the seasonal asymmetries are much weaker in the gravity wave drag patterns. Summer hemisphere anomalies do not weaken as

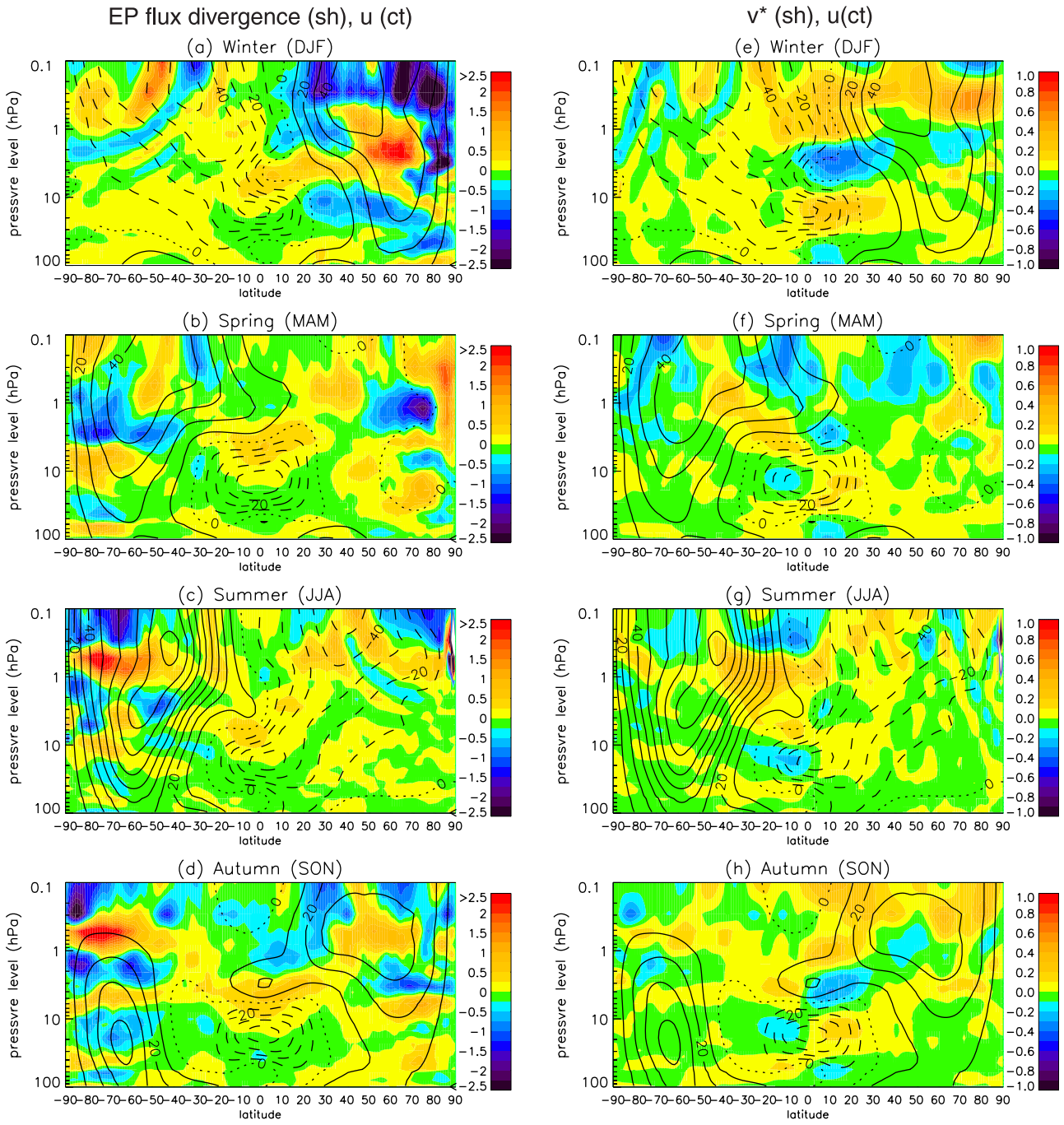

Figure 8. Same as in Figure 6 but for ERA-40 data.

intensely and anomalies in the winter hemisphere do not extend further than 25° of latitude.

[45] Seasonal asymmetries of the QBO signal in the EP flux divergence are also clearly detected in ERA-40 results (Figures 8a, 8b, 8c, and 8d). The patterns are very similar to those obtained with MAECHAM5 data. However, some differences are also found. EP flux divergence anomalies form deeper layers in ERA-40 since QBO zonal wind shear zones are also deeper. Anomalies are also slightly weaker than in MAECHAM5 at all latitudes. As a result, the asymmetric structure of the anomalies in the southern winter, where anomalies are weaker than in northern winter, is not as evident.

[46] It has been mentioned that the previous studies of *Lindzen and Holton* [1968] and *Haynes* [1998] showed that, for the QBO time scale, the eddy forcing has different effects at different latitudes. At low latitudes the response appears primarily as a local acceleration of the zonal wind, but in the extratropics it appears as a meridional circulation. Patterns obtained for the EP flux divergence and v^* are consistent with this behavior. Comparing EP flux divergence and v^* patterns (Figures 6 and 8) it can be seen that residual meridional circulation appears as a response to the

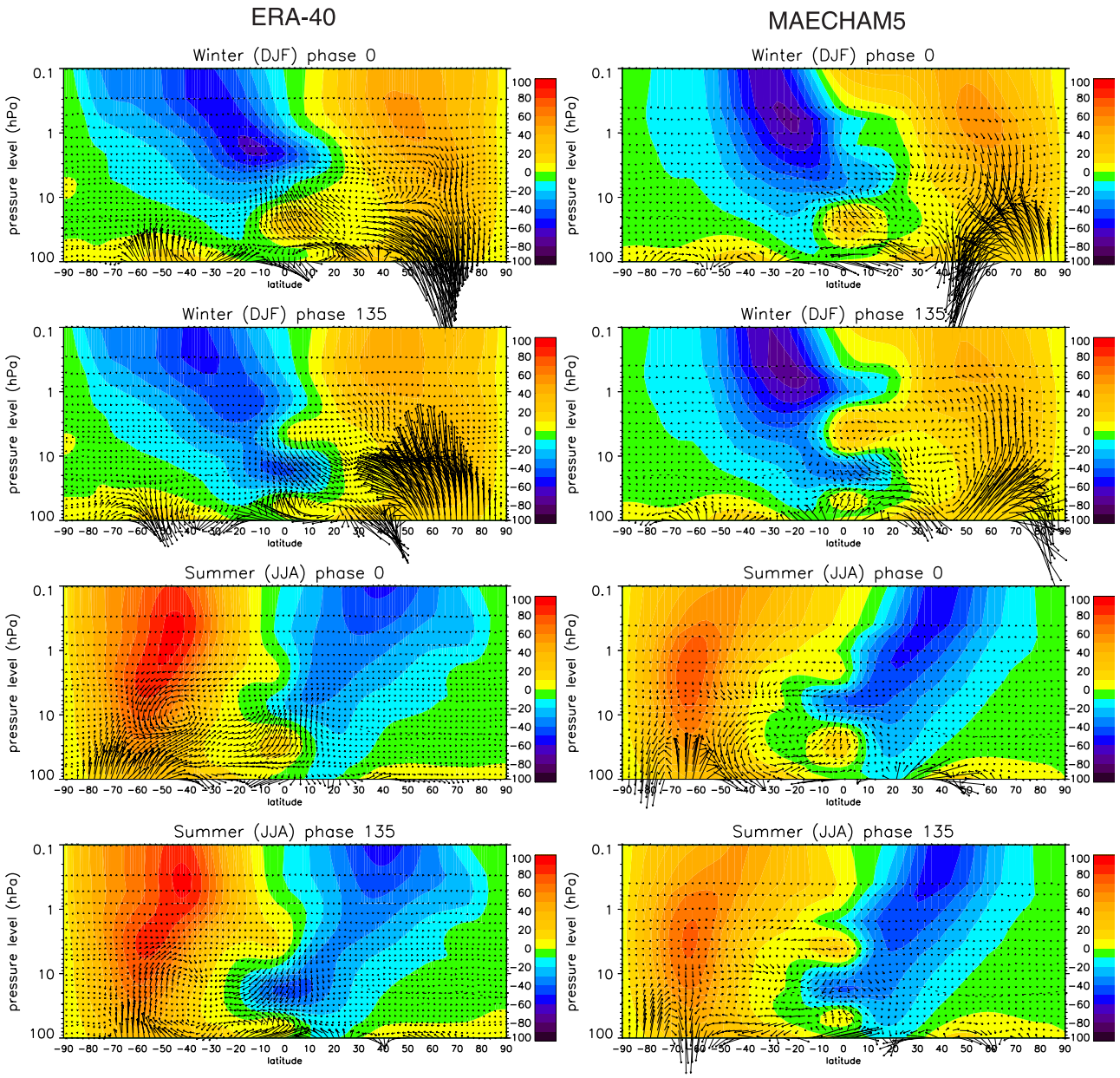

Figure 9. Reconstructed EP flux (arrows, $F_z/F_y = 130$) and total zonal wind field (color scale) patterns associated with 0.40 cycles year^{-1} at phase 0° and 135° for summer and winter seasons and from (left) ERA-40 and (right) MAECHAM5.

eddy forcing as distance from the equator increases and the Coriolis force becomes stronger. In spring and autumn (Figures 6b and 6d for MAECHAM5 and 8b and 8d for ERA-40), when EP flux divergence anomalies associated with the QBO are mostly found in the tropical region, the main response to this forcing is the local acceleration of the zonal wind that generates the QBO. In this region meridional motions are part of the secondary circulation of the QBO (Figures 6f and 6h for MAECHAM5 and 8f and 8h for ERA-40). However, in the winter hemispheres where EP flux divergence anomalies reach middle and high latitudes, meridional circulation appears in the extratropics as a response to this forcing (Figures 6e and 6g for MAECHAM5 and 8e and 8g for ERA-40). Both EP flux divergence and v^* anomalies extend poleward reaching similar latitudes at the same levels and anomalies of both variables increase with height in the same way. On the other hand, anomalies of both variables weaken in the summer hemisphere, especially in the southern summer hemisphere where they almost disappear. It is also shown that, as for the EP flux divergence, v^* anomalies are also weaker in the southern than in the northern winter hemisphere. Continuity conditions explain the strong vertical motions at middle latitudes of the winter hemisphere that complete the asymmetric spatial structure of the secondary circulation.

[47] Results show that the QBO signal in EP flux divergence and the residual meridional circulation extend to the midlatitudes only in the winter hemispheres. This is evi-

dently related to the propagation characteristics of quasi-stationary Rossby waves. These waves can only propagate upward through westerly winds, and for this reason, they are present throughout the stratosphere in the winter hemisphere but not in the summer hemisphere, where easterlies dominate [*Andrews et al.*, 1987]. Typically, the dominant direction of Rossby wave propagation in the winter stratosphere is upward and equatorward. However, the propagation of Rossby waves also depends on the latitudinal-height structure of the tropical zonal wind. As waves reach the tropics they encounter QBO westerlies and easterlies at different levels. At levels where the tropical mean flow is westerly the zero wind line, or critical line, lies on the summer side of the equator at around 5° of latitude. Then the waves are able to penetrate into the tropics and even across the equator without significant dissipation. Coherently, positive EP flux divergence anomalies are found at these levels in the winter subtropics (summer and winter plots in Figures 6 and 8). On the other hand, at the levels with easterly QBO wind, quasi-stationary waves encounter a zero wind line, or critical line, at 20°–30° of latitude on the winter side of the equator, where they would be expected to break. At these levels, the EP flux divergence pattern shows negative anomalies in the winter hemisphere extending to extratropical latitudes (summer and winter plots in Figures 6 and 8) what may be interpreted as an enhancement of the (negative) EP flux divergence resulting from breaking and dissipation of Rossby waves as they encounter the zero wind line. The modulation of EP flux divergence related to Rossby waves is facilitated by the advective shift of the QBO jets to the winter hemisphere described in section 4.2, which is larger toward the northern hemisphere than the southern hemisphere because of the generally larger northern planetary wave activity and hence stronger Brewer Dobson circulation.

[48] Figure 9 represents the zonal mean zonal wind and the QBO signature induced in the EP flux at phase 0° and 135° and for summer and winter seasons. This time the figure represents two different phases of the QBO cycle to better shown how EP flux anomalies are structured in the QBO westerly and easterly layers at different levels. The different behavior of Rossby waves as they reach the QBO easterly or westerly regions is clearly shown in this figure. In the QBO easterly regions EP flux anomalies are directed toward the pole what is consistent with a reduction of the equatorward propagation of Rossby waves and implies a negative anomaly in the divergence of the EP flux in the winter subtropics as observed in Figures 6a and 6c and 8a and 8c. The opposite is found in the QBO westerly regions where equatorward EP flux anomalies means a relative enhancement of the equatorward propagation of Rossby waves consistent with a positive anomaly in the divergence of the EP flux in the winter subtropics as observed in Figures 6a and 6c and 8a and 8c.

[49] Results shown in this section make clear that there are two dynamic processes at work generating a single meridional wind anomaly from the equator to midlatitudes in the winter hemisphere. While the meridional wind anomalies within the QBO jets results from the differential meridional deflection of the zonal wind jets, meridional circulation anomalies at midlatitudes are forced by Rossby wave dissipation being sensitive to the QBO. Both forcings result in meridional wind anomalies of equal signs so that a single meridional wind anomaly can extend from the equatorial latitudes to the midlatitudes of the winter hemispheres. Hence the meridionaly extended secondary circulation of the QBO depends on two different dynamical processes resulting in equal effects in the meridional wind within the QBO domain and in the latitudes extending into the winter hemisphere. For this reason a differentiation should be made between the intrinsic QBO secondary circulation, which results from the presence of the zonally symmetric jets of the QBO, and the extended QBO secondary circulation depending on the presence of extratropical planetary waves. The former tends to be equatorially symmetric (except for nonlinear effects), while the latter necessarily introduces an asymmetry because the mechanism depends on the propagation of extratropical planetary waves to the stratosphere, which depends on season and is different in intensity in the Northern and Southern hemisphere.

5. Conclusions

[50] The secondary circulation of the QBO has been detected and reconstructed from ERA-40 and MAECHAM5 data sets. The patterns obtained for seasonal mean data make evident the strong seasonal dependence of the QBO secondary circulation and describe its spatial structure in the stratosphere and lower mesosphere as a function of latitude and pressure. In agreement with previous studies, the autumn and spring patterns show mass stream function anomalies in the tropics and subtropics that are approximately symmetric about the equator and give rise to a symmetric secondary circulation with a two-cell structure. These anomalies are markedly weaker in the summer hemisphere and stronger in the winter hemisphere, leading to an asymmetric QBO secondary circulation characterized by a single-cell structure displaced into the winter hemisphere. These results provide the first description of the QBO secondary circulation asymmetries throughout the stratosphere and the lower mesosphere in the ERA-40 reanalysis data set. It is also shown that the MAECHAM5 general circulation model correctly reproduces the seasonally asymmetries.

[51] There is a strong seasonal signal in the EP flux divergence anomalies associated with the QBO. During the equinoxes the QBO signal in the EP flux divergence is mainly observed in the tropical region in the shear layers of the QBO and is symmetric about the equator. However, during the solstices it strengthens and reaches middle latitudes in the winter hemisphere while they weaken or disappear from the summer hemisphere. The interaction between Rossby waves and the tropical QBO zonal wind can explain the seasonal asymmetries of the EP flux divergence. In the stratosphere, the wave activity in both hemispheres is similar during autumn and spring. However, planetary Rossby waves of extratropical origin mainly propagate through the winter stratosphere, leading to a strong seasonality in wave fluxes in both hemispheres. At levels where QBO easterlies dominate, the position of the zero wind line in the winter hemisphere reaches latitudes between 20° and 30° in the winter hemisphere. Stronger dissipation of Rossby waves, as they encounter this critical

line, would cause negative EP flux divergence anomalies found at these levels in extratropical latitudes. On the other hand, the EP flux divergence anomalies are positive at levels where westerlies dominate the tropical stratosphere and there is no critical line that could induce strong dissipation of Rossby waves in the winter hemisphere.

[52] Seasonal asymmetries found in the EP flux divergence patterns match very well with those observed in the meridional residual circulation what clearly shows that the seasonal asymmetries in the circulation arises from the asymmetric eddy forcing. The equatorially symmetric eddy forcing observed during the equinoxes gives directly rise to the QBO zonal wind and indirectly also to a symmetric secondary circulation. However, during the solstices EP flux divergence anomalies are stronger and extend to middle latitudes in the winter hemisphere leading to an extension of the anomalies in the meridional circulation. In the extratropical winter hemisphere the dynamic response of the atmosphere to EP flux divergence in the surf zone is a meridional circulation, so that the QBO modulation of the forcing is dynamically transformed to anomalies in the meridional circulation extending across the surf zone. These meridional circulation anomalies occur at the levels of the equatorial zonal wind jets of the QBO, where also the intrinsic QBO secondary circulation arises in the QBO jets. Then, two dynamic processes leading to a single meridional wind anomaly from the equator to midlatitudes in the winter hemisphere can be distinguished. The beta effect is the cause of the intrinsic secondary circulation of the QBO that appears in all seasons. The divergence of EP flux related to the quasi-stationary Rossby waves is the primary driving force of the extended secondary circulation in the winter hemisphere. This divergence generates the extension to the midlatitudes, because (1) the dissipation is sensitive to the QBO wind direction at different layers (2) the resulting effect in the meridional circulation has the same sign as that in the QBO jets. So in the end the single cells extending to the midlatitudes in winter time are combination of the intrinsic QBO secondary circulation and the QBO modulation of the meridional residual circulation.

[53] The excitation of planetary waves differs between the hemispheres because of the different surface properties as orography and land sea distribution. The amplitude of these waves is larger in the northern hemisphere than in the southern hemisphere. The hemispheric differences in Rossby wave activity finally explain the different intensities of the QBO signal in the meridional wind anomalies, i.e., the stronger asymmetry of the QBO secondary circulation in the northern winter hemisphere.

[54] *Kinnersley* [1999] used an idealized 2-D model, in which two processes are investigated: the solsticial cross equatorial advection, and friction damping westerlies, an idealized method to represent the effects of breaking planetary waves. The mechanism proposed by Kinnersley to explain the seasonal asymmetries of the QBO secondary circulation was based on the meridional advection of the QBO zonal wind anomalies into the winter hemisphere by the Brewer-Dobson circulation. In this way, he could explain the seasonal asymmetries without invoking any interaction between the zonal wind and Rossby waves. However, he showed that when friction was applied to the zonal wind in the winter hemisphere, the QBO secondary circulation spreads to middle latitudes in the winter hemisphere. He suggested that friction works in two different ways to cause the spreading: damping the QBO zonal wind and its vertical gradient which implies latitudinal spreading of the temperature and vertical wind anomalies and also, increasing the meridional flow and then the advection of the QBO jets into the winter hemisphere. In this study we detect and quantify seasonal asymmetries in the EP flux divergence anomalies associated with the QBO in MAECHAM5, that represents a realistic QBO and planetary waves and also from the ERA-40, which include a realistic QBO and planetary waves because of the observations analyzed in the IFS (Integrated Forecasting System) model. Stronger (weaker) dissipation of Rossby waves in the subtropics at the levels where QBO easterlies (westerlies) dominate in the tropical region give rise to an extratropical extension of the EP flux divergence anomalies associated with the QBO. At the extratropics, these forcings are balanced by a meridional circulation that extends the direct circulation of the QBO to the midlatitudes. These results allow us to suggest that seasonal asymmetries of the extended secondary circulation are forced by Rossby wave dissipation being sensitive to the QBO. Meridional advection of the QBO jets toward the winter hemisphere, however, facilitates the QBO modulation of the EP flux of Rossby waves.

[55] **Acknowledgments.** This work was partly funded by the Spanish National Research Project TRODIM MEC-CGL2007-65891-C05-04-CLI.

References

Andrews, D. G., and M. E. McIntyre (1976), Planetary waves in horizontal and vertical shear: The generalized Eliassen-Palm relation and the mean zonal acceleration, *J. Atmos. Sci.*, *33*, 2031–2048.

Andrews, D. G., J. R. Holton, and C. B. Leovy (1987), *Middle Atmosphere Dynamics*, 489 pp., Academic, San Diego, Calif.

Baldwin, M. P., and L. J. Gray (2005), Tropical stratospheric winds in ECMWF ERA-40 reanalysis, rocketsonde data, and rawinsonde data, *Geophys. Res. Lett.*, *32*(9), L09806, doi:10.1029/2004GL022328.

Baldwin, M. P., et al. (2001), The quasi-biennial oscillation, *Rev. Geophys.*, *39*, 179–229.

Bengtsson, L., K. I. Hodges, and S. Hagemann (2004), Sensitivity of the ERA40 reanalysis to the observing system: Determination of the global atmospheric circulation from reduced observations, *Tellus*, *56A*, 456–471.

Calvo, N., M. A. Giorgetta, and C. Pena-Ortiz (2007), Sensitivity of the boreal winter circulation in the middle atmosphere to the quasi-biennial oscillation in MAECHAM5 simulations, *J. Geophys. Res.*, *112*, D10124, doi:10.1029/2006JD007844.

Dunkerton, T. J. (1985), A two-dimensional model of the quasi-biennial oscillation, *J. Atmos. Sci.*, *42*, 1151–1160.

Dunkerton, T. J. (1997), The role of gravity waves in the quasibiennial oscillation, *J. Geophys. Res.*, *102*, 26,053–26,076.

Dunkerton, T. J., and D. P. Delisi (1985), Climatology of the equatorial lower stratosphere, *J. Atmos. Sci.*, *42*, 376–396.

Dunkerton, T. J., and D. P. Delisi (1997), Interaction of the quasi-biennial oscillation and stratopause semiannual oscillation, *J. Geophys. Res.*, *102*, 26,107–26,116.

Efron, B. (1990), More efficient bootstrap computations, *J. Am. Stat. Assoc.*, *85*(409), 79–89.

Garcia, R. R. (1987), On the mean meridional circulation of the middle atmosphere, *J. Atmos. Sci.*, *44*, 3599–3609.

Giorgetta, M. A., E. Manzini, and E. Roeckner (2002), Forcing of the quasi-biennial oscillation from a broad spectrum of atmospheric waves, *Geophys. Res. Lett.*, *29*(8), 1245, doi:10.1029/2002GL014756.

Giorgetta, M. A., E. Manzini, E. Roeckner, M. Esch, and L. Bengtsson (2006), Climatology and forcing of the quasi-biennial oscillation in the MAECHAM5 model, *J. Clim.*, *19*(16), 3882–3901.

Hamilton, K. (1998), Effects of an imposed quasi-biennial oscillation in a comprehensive troposphere-stratosphere-mesosphere general circulation model, *J. Atmos. Sci.*, *55*, 2393–2418.

Haynes, P. H. (1998), The latitudinal structure of the quasi-biennial oscillation, *Q. J. R. Meteorol. Soc.*, *124*, 2645–2670.

Holton, J. R. (1989), Influence of the annual cycle in meridional transport on the quasi-biennial oscillation in total ozone, *J. Atmos. Sci.*, *46*, 1434–1439.

Holton, J. R., and H. C. Tan (1980), Influence of the equatorial quasi-biennial oscillation on the global circulation at 50 Mb, *J. Atmos. Sci.*, *37*(10), 2200–2208.

Huesmann, A. S., and M. H. Hitchman (2001), The stratospheric quasi-biennial oscillation in the NCEP reanalyses: Climatological structures, *J. Geophys. Res.*, *106*, 11,859–11,874.

Jones, D. B. A., H. R. Schneider, and M. B. McElroy (1998), Effects of the quasi-biennial oscillation on the zonally averaged transport of tracers, *J. Geophys. Res.*, *103*, 11,235–11,249.

Kinnersley, J. S. (1999), On the seasonal asymmetry of the lower and middle latitude QBO circulation anomaly, *J. Atmos. Sci.*, *56*, 1140–1153.

Kinnersley, J. S., and K. K. Tung (1999), Mechanisms for the extratropical QBO in circulation and ozone, *J. Atmos. Sci.*, *56*(12), 1942–1962.

Lindzen, R. S., and J. R. Holton (1968), A theory of the quasi-biennial oscillation, *J. Atmos. Sci.*, *25*, 1095–1107.

Mann, M. E., and J. Park (1999), Oscillatory patio-temporal signal detection in climate studies: A multiple-taper spectral domain approach, *Adv. Geophys.*, *41*, 1–131.

Manzini, E., M. A. Giorgetta, M. Esch, L. Kornblueh, and E. Roeckner (2006), The influence of sea surface temperatures on the Northern winter stratosphere: Ensemble simulations with the MAECHAM5 model, *J. Clim.*, *19*, 3863–3881.

Pascoe, C. L., L. J. Gray, S. A. Crooks, M. N. Juckes, and M. P. Baldwin (2005), The quasi-biennial oscillation: Analysis using ERA-40 data, *J. Geophys. Res.*, *110*, D08105, doi:10.1029/2004JD004941.

Plumb, R. A. (1984), The quasi-biennial oscillation, in *Dynamics of the Middle Atmosphere*, edited by J. R. Holton and T. Matsuno, pp. 217–251, Terra Sci., Tokyo, Japan.

Plumb, R. A., and R. C. Bell (1982), A model of the quasi-biennial oscillation on an equatorial beta-plane, *Q. J. R. Meteorol. Soc.*, *108*, 335–352.

Punge, H. J., and M. A. Giorgetta (2007), Differences between the QBO in the first and in the second half of the ERA-40 reanalysis, *Atmos. Chem. Phys.*, *7*, 599–608.

Reed, R. J. (1964), A tentative model of the 26-month oscillation in tropical latitudes, *Q. J. R. Meteorol. Soc.*, *90*, 441–466.

Ribera, P., D. Gallego, C. Pena-Ortiz, L. Gimeno, R. Garcia-Herrera, E. Hernandez, and N. Calvo (2003), The stratospheric QBO signal in the NCEP reanalysis 1958-2001, *Geophys. Res. Lett.*, *30*(13), 1691, doi:10.1029/2003GL017131.

Ribera, P., C. Pena-Ortiz, R. Garcia-Herrera, D. Gallego, L. Gimeno, and E. Hernandez (2004), Detection of the secondary meridional circulation associated with the quasi-biennial oscillation, *J. Geophys. Res.*, *109*, D18112, doi:10.1029/2003JD004363.

Roeckner, E., et al. (2003), The atmospheric general circulation model ECHAM5. part 1, *MPI-Rep. 349*, 127 pp.

Roeckner, E., R. Brokopf, M. Esch, M. Giorgetta, S. Hagemann, L. Kornblueh, E. Manzini, U. Schlese, and U. Schulzweida (2006), Sensitivity of simulated climate to horizontal and vertical resolution in the ECHAM5 atmosphere model, *J. Clim.*, *19*, 3771–3791.

Ruzmaikin, A., J. Feynman, and X. Jiang (2005), Extratropical signature of the quasi-biennial oscillation, *J. Geophys. Res.*, *110*, D11111, doi:10.1029/2004JD005382.

Takahashi, M. (1987), A two-dimensional numerical model of the quasi-biennial oscillation, *J. Meteorol. Soc. Jpn.*, *65*, 523–535.

Tung, K., and H. Yang (1994), Global QBO in circulation and ozone. part II: A simple mechanistic model, *J. Atmos. Sci.*, *51*, 2708–2721.

Uppala, S. M., et al. (2005), The ERA-40 re-analysis, *Q. J. R. Meteorol. Soc.*, *131*, 2961–3012, doi:10.1256/qj.04.176.

R. R. García, Atmospheric Chemistry Division, National Center for Atmospheric Research, P.O. Box 3000, Boulder, CO 80307-3000, USA.

R. García-Herrera, Departamento de Física de la Tierra II, Facultad de CC Físicas, Universidad Complutense de Madrid, 28040 Madrid, Spain.

M. A. Giorgetta, Department of Atmosphere in Earth System, Max Planck Institute for Meteorology, Hamburg, Germany.

C. Peña-Ortiz and P. Ribera, Departamento de Sistemas Fisicos, Quimicos y Naturales, Universidad Pablo de Olavide, Carretera de Utreta, km 1, 41013 Sevilla, Spain. (cpenort@upo.es)